

Jet formation in BL Lacertae objects with different accretion modes

Xinwu Cao

*Shanghai Astronomical Observatory, Chinese Academy of Sciences, 80 Nandan Road,
Shanghai, 200030, China
Email: cxw@center.shao.ac.cn*

ABSTRACT

We estimate the masses of massive black holes in BL Lac objects from their host galaxy luminosity. The power of jets and central optical ionizing luminosity for a sample of BL Lac objects are derived from their extended radio emission and the narrow-line emission, respectively. The maximal jet power can be extracted from a standard thin accretion disk/spinning black hole is calculated as a function of dimensionless accretion rate \dot{m} ($\dot{m} = \dot{M}/\dot{M}_{\text{Edd}}$). Comparing with the derived jet power, we find that the accretion disks in most BL Lac objects should not be standard accretion disks. For a pure advection dominated accretion flow (ADAF), there is an upper limit on its optical continuum luminosity due to the existence of an upper limit \dot{m}_{crit} on the accretion rate. It is found that a pure ADAF is too faint to produce the optical ionizing luminosity of BL Lac objects derived from their narrow-line luminosity. We propose that an ADAF is present in the inner region of the disk and it becomes a standard thin disk in the outer region in most BL Lac objects, i.e., ADAF+SD(standard disk) scenario. This ADAF+SD scenario can explain both the jet power and optical ionizing continuum emission of these BL Lac objects. The inferred transition radii between the inner ADAF and outer SD are in the range of $40 - 150 GM_{\text{bh}}/c^2$, if the disks are accreting at the rate $\dot{m} = 0.01$.

Subject headings: galaxies: active—BL Lacertae objects: general—galaxies: jets—accretion, accretion disks—black hole physics

1. Introduction

Most BL Lac objects have featureless optical and ultraviolet continuum spectra, and only a small fraction of BL Lac objects show very weak broad emission lines (Veron-Cetty & Veron 2000). The low-energy-peaked BL Lac(LBL) objects exhibit similar radio and optical continua as flat-spectrum radio quasars (FSRQ) (Urry & Padovani 1995). Similar to other quasars, FSRQs have strong broad-line emission. The broad emission lines of quasars are produced by the optical/UV continua reprocessed by distant gas clouds in broad-line regions (BLRs). The optical/UV continuum emission ionizing the gases in BLRs is believed to be from the accretion disks surrounding massive black holes (Sun & Malkan 1989). Low accretion rates \dot{m} may lead the accretion flows to be advection dominated (Narayan & Yi 1995). The emission from an ADAF is very faint due to its low radiative efficiency and low accretion rate. Also, low gas densities are expected in their environment for low accretion rates \dot{m} . These can account for the feature of no emission lines (or very weak) in BL Lac objects naturally if their accretion disks are accreting at low rates \dot{m} . For some individual BL Lac objects, it is found that the accretion rates are indeed very low, for example, $L_{\text{bol}}/L_{\text{Edd}} \sim 10^{-4}$ for Mkn501 (Barth, Ho, & Sargent 2002). Cavaliere & D’Elia (2002) proposed that advection dominated accretion flows (ADAFs) may be present in most BL Lac objects. They suggested a possible evolutionary sequence for blazars. The detailed calculations on the spectra of the ADAFs indicate that most BL Lac objects may have ADAFs surrounding their massive black holes (Cao 2002a). On the other hand, FR I radio galaxies are believed to be the misaligned BL Lac objects in the frame of unification schemes of active galactic nuclei (AGNs) (see Urry & Padovani 1995 for a review). Chiaberge, Capetti, & Celotti (1999) estimated the upper limits of the disk emission of FR I radio galaxies from the observed optical core fluxes and found that the optical core luminosity of FR I radio galaxies is far lower than the Eddington one L_{Edd} , typically $\lambda L_{\text{c,opt}}/L_{\text{Edd}} \leq 10^{-4}$, if the black holes in FR I radio galaxies are around $10^9 M_{\odot}$. Ghisellini & Celotti (2001) used the optical luminosity of the host galaxy to estimate the central black hole mass of FR I radio galaxy. The central ionizing luminosity is estimated from the power of jets in FR I galaxies. They found that almost all FR I radio galaxies are accreting at very low rates: $\dot{m} \leq 0.001 - 0.01$.

Relativistic jets have been observed in many BL Lac objects and FSRQs, which are believed to be formed very close to the black holes. The spin energy of a black hole might be extracted to power the jet by magnetic fields supported by a surrounding accretion disk (the Blandford-Znajek mechanism; Blandford & Znajek 1977). This process has been widely regarded as the major mechanism that powers radio jets in AGNs (Begelman, Blandford, & Rees 1984; Rees et al. 1982; Wilson & Colbert 1995; Moderski & Sikora 1996). However, Ghosh & Abramowicz (1997) doubted the importance of the Blandford-Znajek process. For a black hole of a given mass and angular momentum, the strength of the Blandford-Znajek

process depends crucially on the strength of the poloidal field threading the horizon of the hole. The magnetic field threading a hole should be maintained by the currents situated in the inner region of the surrounding accretion disk. They argued that the strength of the field threading a black hole has been overestimated. Livio, Ogilvie, & Pringle (1999; hereafter L99) re-investigated the problem and pointed out that even the calculations of Ghosh & Abramowicz (1997) have overestimated the power of the Blandford-Znajek process, since they have overestimated the strength of the large-scale field threading the inner region of an accretion disk, and then the power of the Blandford-Znajek process. The strength of the large-scale field scales with the disk thickness, and it is very weak if the field created by dynamo processes for thin disk cases. L99 estimated the maximal jet power extracted from an accretion disk on the assumption that the toroidal field component is of the same order of the poloidal field component at the disk surface. They argued that the maximal jet power extracted from an accretion disk (the Blandford-Payne mechanism; Blandford & Payne 1982) dominates over the maximal power extracted by the Blandford-Znajek process (L99). Apart from the strength of the field threading a disk, the acceleration of the jet is also governed by the magnetic field configuration and the structure of the disk (Shu 1991; Ogilvie & Livio 1998, 2001; Cao & Spruit 2002). It is unclear how much power can actually be extracted from a magnetized accretion disk without considering its large-scale field configuration (Cao 2002b).

In this paper, we use a sample of low-energy-peaked BL Lac objects to explore the jet formation in BL Lac objects. The cosmological parameters $H_0 = 50 \text{ km s}^{-1} \text{ Mpc}^{-1}$ and $q_0 = 0.5$ have been adopted in this work.

2. Sample

Urry et al. (2000) used the Hubble Space Telescope (HST) WFPC2 camera to survey 132 BL Lac objects. The host galaxies of 80 BL Lac objects are detected, among which there are 29 LBLs. We use these 29 sources as our sample to study the jet formation in BL Lac objects. We search the literature and find extended radio emission data of these sources except 0454+844. We use the luminosity of the narrow-line [O II] at 3727 Å to estimate the optical ionizing luminosity. For those the emission data of [O II] being unavailable, we estimate the [O II] emission from other emission lines adopting the line ratio proposed by Francis et al. (1991). The narrow-line emission data is available for 22 sources in this sample. The data are listed in Table 1.

3. Black hole mass

In order to estimate the central black hole masses of BL Lac objects, we use the relation between host galaxy absolute magnitude M_R at R -band and black hole mass M_{bh} proposed by McLure & Dunlop (2002)

$$\log_{10}(M_{\text{bh}}/M_{\odot}) = -0.50(\pm 0.02)M_R - 2.96(\pm 0.48). \quad (1)$$

The black hole masses of some sources in our sample have already been estimated from their stellar dispersion velocity by using $M_{\text{bh}} - \sigma$ relation (Ferrarese & Merritt 2000; Gebhardt et al. 2000). The estimated black hole masses from the stellar dispersion velocity are: $\log(M_{\text{bh}}/M_{\odot}) = 8.65(0521-365)$, $8.51(1807+698)$, and $8.10(2201+044)$ (Barth, Ho, & Sargent 2003). Falomo, Kotilainen, & Treves (2002) estimated the black hole masses in the same way: $\log(M_{\text{bh}}/M_{\odot}) = 8.90(1807+698)$, and $8.27(2201+044)$. These results agree fairly well with the black hole masses estimated in this paper from the host galaxy luminosity: $\log(M_{\text{bh}}/M_{\odot}) = 8.68(0521-365)$, $9.00(1807+698)$, and $8.32(2201+044)$ (see Table 1).

4. Jet power

The relation between jet power and radio luminosity proposed by Willott et al. (1999) is

$$Q_{\text{jet}} \simeq 3 \times 10^{38} f^{3/2} L_{\text{ext},151}^{6/7} \text{ W}, \quad (2)$$

where $L_{\text{ext},151}$ is the extended radio luminosity at 151 MHz in units of $10^{28} \text{ W Hz}^{-1} \text{ sr}^{-1}$. Willott et al. (1999) have argued that the normalization is very uncertain and introduced the factor f to account for these uncertainties. They use a wide variety of arguments to suggest that $1 \leq f \leq 20$. In this paper, we adopted the low limit $f = 1$ in most cases. This relation was proposed for FR II radio galaxies and quasars. We adopt this relation to estimate the power of jets in BL Lac objects which is believed to be a good approximation, since BL Lac objects have similar radio properties as radio quasars. For most BL Lac objects, their radio/optical continuum emission is strongly beamed to us due to their relativistic jets and small viewing angles of the jets with respect to the line of sight (e.g. Fan 2003). The low-frequency radio emission (e.g. 151 MHz) may still be Doppler beamed. We therefore use the extended radio emission detected by VLA to estimate the jet power. The observed extended radio emission is K -corrected to 151 MHz in the rest frame of the source assuming $\alpha_e = 0.8$ ($f_{\nu} \propto \nu^{-\alpha_e}$) (Chiaberge, Capetti, & Celotti 1999).

5. Jet formation mechanisms

L99 have calculated the maximal jet power can be extracted from a rapidly spinning black hole/magnetized accretion disk. Our calculations mainly follow L99’s spirit, but in more detail.

5.1. Thin disks

The maximal power of the jet accelerated by an magnetized accretion disk is

$$L_{\text{BP}}^{\text{max}} = 4\pi \int \frac{B_{\text{pd}}^2}{4\pi} R^2 \Omega(R) dR, \quad (3)$$

where $B_{\text{pd}} \sim B_\varphi$ is assumed, and B_{pd} is the strength of the large-scale ordered field at the disk surface.

The origin of the ordered field that is assumed to thread the disk is still unclear. An instability may arise if a strong jet is accelerated by the large-scale field of the disk advected in by the accretion flow (Lubow, Papaloizou, & Pringle 1994; Cao & Spruit 2002). The strength of the field at the disk surface is usually assumed to scale with the pressure of the disk, as done in Ghosh & Abramowicz (1997). However, L99 pointed out that the large-scale field can be produced from the small-scale field created by dynamo processes as $B(\lambda) \propto \lambda^{-1}$ for the idealized case, where λ is the length scale of the field (Tout & Pringle 1996; Romanova et al. 1998). So, the large-scale field threading the disk is related with the field produced by dynamo processes approximately by (L99)

$$B_{\text{pd}} \sim \frac{H}{R} B_{\text{dynamo}}. \quad (4)$$

The scale-height of the disk H/R is given by (Laor & Netzer 1989)

$$\frac{H}{R} = 15.0 \dot{m} r^{-1} c_2, \quad (5)$$

where the coefficient c_2 is defined in Novikov & Thorne (1973, hereafter NT73), and the dimensionless quantities are defined by

$$r = \frac{R}{R_{\text{G}}}, \quad R_{\text{G}} = \frac{GM_{\text{bh}}}{c^2}, \quad \dot{m} = \frac{\dot{M}}{\dot{M}_{\text{Edd}}},$$

and

$$\dot{M}_{\text{Edd}} = \frac{L_{\text{Edd}}}{\eta_{\text{eff}} c^2} = 1.39 \times 10^{15} m \text{ kg s}^{-1}, \quad m = \frac{M_{\text{bh}}}{M_{\odot}} \quad (6)$$

where $\eta_{\text{eff}} = 0.1$ is adopted.

The dimensionless scale-height of a disk H/R is in principle a function of R , and it reaches a maximal value in the inner region of the disk (Laor & Netzer 1989). We adopt the maximal value of H/R in the estimate of large-scale field strength B_{pd} at the disk surface as done by Cao (2002b).

As L99, the strength of the magnetic field produced by dynamo processes in the disk is given by

$$\frac{B_{\text{dynamo}}^2}{4\pi} \sim \frac{W}{2H}, \quad (7)$$

where W is the integrated shear stress of the disk, and H is the scale-height of the disk. For a relativistic accretion disk, the integrated shear stress is given by Eq. (5.6.14a) in NT73. Equation (7) can be re-written as

$$B_{\text{dynamo}} = 3.56 \times 10^8 r^{-3/4} m^{-1/2} A^{-1} B E^{1/2} \text{gauss}, \quad (8)$$

where A , B and E are general relativistic correction factors defined in NT73.

In standard accretion disk models, the angular velocity of the matter in the disk is usually very close to Keplerian velocity. For a relativistic accretion disk surrounding a rotating black hole, the Keplerian angular velocity is given by

$$\Omega(r) = 2.034 \times 10^5 \frac{1}{m(r^{3/2} + a)} \text{ s}^{-1}, \quad (9)$$

where a is dimensionless specific angular momentum of a rotating black hole.

We use Eqs. (4)–(9), the maximal power of the jet accelerated from a magnetized disk is available by integrating Eq. (3), if some parameters: m , \dot{m} , a , are specified.

As discussed in L99, the power extracted from a rotating black hole by the Blandford-Znajek process is determined by the hole mass m , the spin of the hole a , and the strength of the poloidal field threading the horizon of a rotating hole B_{ph} :

$$L_{\text{BZ}}^{\text{max}} = \frac{1}{32} \omega_{\text{F}}^2 B_{\perp}^2 R_{\text{h}}^2 c a^2, \quad (10)$$

for a black hole of mass m and dimensionless angular momentum a , with a magnetic field B_\perp normal to the horizon at R_h . Here the factor $\omega_F^2 \equiv \Omega_F(\Omega_h - \Omega_F)/\Omega_h^2$ depends on the angular velocity of field lines Ω_F relative to that of the hole, Ω_h . In order to estimate the maximal power extracted from a spinning black hole, we adopt $\omega_F = 1/2$. As the field B_\perp is maintained by the currents in the accretion disk surrounding the hole, the strength of B_\perp should be of the same order of that in the inner edge of the disk, and $B_\perp \simeq B_{\text{pd}}(r_{\text{in}})$ is therefore adopted.

5.2. Advection dominated accretion flows

In the case of an ADAF surrounding a rapidly spinning black hole, the maximal jet power extracted by the Blandford-Znajek mechanism was calculated by Armitage & Natarajan (1999). Here, we calculate the jet power in a similar way as done in the last sub-section.

The pressure of an ADAF is given by Narayan & Yi (1995)

$$p = 1.71 \times 10^7 \alpha^{-1} c_1^{-1} c_3^{1/2} m^{-1} \dot{m} r^{-5/2} \text{N m}^{-2}, \quad (11)$$

where α is the viscosity parameter, c_1 and c_3 are given in Narayan & Yi (1995)

$$c_1 = \frac{(5 + 2\epsilon')}{3\alpha^2} g(\alpha, \epsilon') \quad (12)$$

and

$$c_3 = \frac{2(5 + 2\epsilon')}{9\alpha^2} g(\alpha, \epsilon'). \quad (13)$$

Two parameters ϵ' and $g(\alpha, \epsilon')$ are

$$\epsilon' = \frac{1}{f_{\text{adv}}} \left(\frac{5/3 - \gamma}{\gamma - 1} \right) \quad (14)$$

and

$$g(\alpha, \epsilon') = \left[1 + \frac{18\alpha^2}{(5 + 2\epsilon')^2} \right]^{1/2} - 1, \quad (15)$$

where the parameter f_{adv} , which lies in the range 0–1, is the fraction of viscously dissipated energy which is advected; γ is the ratio of specific heats. So, the value of the parameter ϵ' is in the range of 0–1. As done by Armitage & Natarajan (1999), we assume $p_{\text{mag}} \sim \alpha p$, and two parameters $\alpha = 1$ and $\epsilon' = 1$ are adopted to maximize the pressure (see Cao & Rawlings 2003 for detailed calculations). As the accretion rate of an ADAF should be less than the critical one \dot{m}_{crit} , we can calculate the maximal jet power extracted from a spinning black hole of mass m and dimensionless angular momentum a from Eq. (10) assuming $B_\perp \simeq B$, if $\dot{m} = \dot{m}_{\text{crit}}$ is substituted into Eq. (11). The results of the extreme case for $a = 1$ have already been given in Armitage & Natarajan (1999).

6. Spectra of the disks

For normal bright AGNs, the bolometric luminosity can be estimated from their optical luminosity by (Kaspi et al. 2000)

$$L_{\text{bol}} \simeq 9\lambda L_{\lambda, \text{opt}}, \quad (16)$$

which may not be valid for the cases of ADAFs.

For BL Lac objects, the observed optical continuum emission may be dominated by the beamed synchrotron emission from the relativistic jets. We use narrow-line emission to estimate the ionizing luminosity that is believed to be photo-ionized by the disk emission (Rawlings & Saunders 1991). The ionizing luminosity of BL Lac objects can also be derived from their broad-line emission (e.g., Cao 2002a, Wang, Staubert, & Ho, 2002). Here we use the equivalent width of the line [O II]: $\text{EW} = 10\text{\AA}$, corresponding to the ionizing continuum emission (Willott et al. 1999). Thus, we can use relation (16) to estimate the bolometric luminosity of the disks in BL Lac objects from their narrow-line luminosity $L_{[\text{O II}]}$. However, the situation becomes quite different for those sources in which ADAFs are present, because the spectral energy distributions of ADAFs are significantly different from that of standard accretion disks (Mahadevan 1997). Cao (2002a) have calculated the maximal optical luminosity of BL Lac objects for the pure ADAF case, and the lower limits on the central black hole masses of BL Lac objects are derived from their broad-line emission. Here, we consider a more general case, i.e., an ADAF is present near the black hole and it transits to a cold standard disk (SD) beyond the transition radius r_{tr} (Esin, McClintock, & Narayan 1997).

The flux due to viscous dissipation in the outer region of the disk is

$$F_{\text{vis}}(R) \simeq \frac{3GM_{\text{bh}}\dot{M}}{8\pi R^3}, \quad (17)$$

which is a good approximation for $R_{\text{tr}} \gg R_{\text{in}}$. The local disk temperature of the thin cold disk is

$$T_{\text{disk}}(R) = \frac{F_{\text{vis}}(R)^{1/4}}{\sigma_{\text{B}}^{1/4}}, \quad (18)$$

by assuming local blackbody emission. In order to calculate the disk spectrum, we include an empirical color correction for the disk thermal emission as a function of radius. The correction has the form (Chiang 2002)

$$f_{\text{col}}(T_{\text{disk}}) = f_{\infty} - \frac{(f_{\infty} - 1)(1 + \exp(-\nu_{\text{b}}/\Delta\nu))}{1 + \exp((\nu_{\text{p}} - \nu_{\text{b}})/\Delta\nu)}, \quad (19)$$

where $\nu_{\text{p}} \equiv 2.82k_{\text{B}}T_{\text{disk}}/h$ is the peak frequency of a blackbody with temperature T_{disk} . This expression for f_{col} goes from unity at low temperatures to f_{∞} at high temperatures with a

transition at $\nu_b \approx \nu_p$. Chiang (2002) found that $f_\infty = 2.3$ and $\nu_b = \Delta\nu = 5 \times 10^{15}$ Hz do a reasonable job of reproducing the model disk spectra of Hubeny et al. (2001). The disk spectra can therefore be calculated by

$$L_\nu = 8\pi^2 \left(\frac{GM}{c^2} \right)^2 \frac{h\nu^3}{c^2 f_{\text{col}}^4} \int_{r_{\text{tr}}}^{\infty} \frac{r dr}{\exp(h\nu/f_{\text{col}} k_B T_{\text{disk}}) - 1}. \quad (20)$$

In this ADAF+SD scenario, the ionizing luminosity from the disk is a combination of the emission from the inner ADAF and outer standard disk regions. Cao (2002a)’s calculations indicate that the optical continuum emission from the inner ADAF region can be neglected compared with that from outer SD region if r_{tr} is around tens to several hundreds, which is due to the low radiation efficiency of ADAFs.

7. Results

In Fig. 1, we plot the relation between the ratios $L_{\text{bol}}/L_{\text{Edd}}$ and $Q_{\text{jet}}/L_{\text{bol}}$. For a standard thin disk, The optical luminosity of BL Lac objects is estimated from their narrow-line luminosity $L_{[\text{O II}]}$ by assuming $\text{EW} = 10\text{\AA}$. We convert the optical luminosity to bolometric luminosity using the relation (16). The black hole masses of BL Lac objects are estimated by using the relation (1) from the host galaxy luminosity. The ratio $L_{\text{bol}}/L_{\text{Edd}}$ is then available. The jet power of BL Lac objects is estimated from the low-frequency extended radio luminosity by using the relation (2).

For a standard thin disk, we can calculate the maximal jet power $L_{\text{BP}}^{\text{max}}$ extracted from the magnetized accretion disk as functions of black hole mass m and accretion rate \dot{m} using Eqs. (3), (4), and (8). In a similar way, the maximal jet power $L_{\text{BZ}}^{\text{max}}$ extracted from a spinning hole is also calculated from Eqs. (4), (8), and (10), if the black hole mass m and dimensionless black hole angular momentum a are specified. The ratios $L_{\text{bol}}/L_{\text{Edd}}$ and $Q_{\text{jet}}/L_{\text{bol}}$ are functions of the accretion rate \dot{m} and black hole spin a . We vary accretion rate \dot{m} and then the relations of $L_{\text{BP}}^{\text{max}}/L_{\text{bol}}$ and $L_{\text{BZ}}^{\text{max}}/L_{\text{bol}}$ with $L_{\text{bol}}/L_{\text{Edd}}$ are calculated for $a = 0.95$ (see Fig. 1). We find that the jet power of most sources in our sample is above the maximal jet power expected to be extracted from a magnetized accretion disk (above the solid line in Fig. 1). All sources have jet power much higher than the maximal jet power extracted by the Blandford-Znajek mechanism (above the dotted line). This implies that only the jets in three sources: 0828+493, 0851+202, and 2240–260 (labelled squares in Fig. 1, hereafter referred as square sources) may be fuelled by the magnetized thin disks, and no jet in the sources of this sample can be powered only by the Blandford-Znajek mechanism, if the standard thin accretion disks are present in these sources.

We plot the relation of jet power Q_{jet} with black hole mass M_{bh} in Fig. 2. All sources have jet power less than $0.01 L_{\text{Edd}}$. The exact value of the critical accretion rate \dot{m}_{crit} is still unclear for an ADAF, which depends on the value of the disk viscosity parameter α . For AGNs, the value of the critical accretion rate \dot{m}_{crit} is probably around ~ 0.01 (Narayan 2002). The maximal jet power extracted from a rapidly spinning black hole $a = 0.95$ is calculated as a function of black hole mass M_{bh} assuming $\dot{m}_{\text{crit}} = 0.01$.

The relation between black hole mass M_{bh} and the central optical ionizing continuum luminosity L_{λ} at 3727 \AA is plotted in Fig. 3. The optical continuum emission from a pure ADAF can be calculated by using the approach proposed by Mahadevan (1997). We use the same approach proposed by Cao (2002a) to calculate the maximal optical continuum emission from an ADAF as a function of black hole mass M_{bh} . The maximal optical continuum emission requires the parameter $\beta = 0.5$, which describes the magnetic field strength with respect to gas pressure, and viscosity $\alpha = 1$. Changing the value of accretion rate \dot{m} , we can find the maximal optical continuum luminosity for given black hole mass (see Cao, 2002a for details). It is found that all sources have optical ionizing luminosity higher than the maximal optical luminosity expected from pure ADAFs, which implies that the emission from pure ADAFs is unable to explain the optical ionizing luminosity of these sources. The optical spectra of the standard accretion disks are also calculated for different accretion rates $\dot{m} = 0.001, 0.01$, and 0.1 , respectively. Most sources, except three square sources, have optical ionizing luminosity below the line of $\dot{m} = 0.01$ expected from the standard disk. We further calculate the optical spectra of ADAF+SD systems as described in Sect. 6, for different values of transition radius r_{tr} . All these sources lie in the region between $r_{\text{tr}} = 40$ and 150 for $\dot{m} = 0.01$. If $\dot{m} = 0.1$ is adopted, the transition radii of the disks are required to be in the range of $100 - 400$ to explain the optical ionizing emission.

In Figs. 4 and 5, we present the results as that in Figs. 1 and 2, but for $f = 10$ is adopted in the normalization of the jet power estimate (2).

8. Discussion

For a standard magnetized accretion disk, the strength of the large-scale ordered field of the disk is related with the scale-height of the disk. The scale-height of the disk is proportional to dimensionless accretion rate \dot{m} . Thus, the maximal jet power extracted from the disk or the spinning black hole depends on the accretion rate \dot{m} . We found that only three sources $0828 + 493$, $0851 + 202$, and $2240 - 260$ have lower jet power than the maximal jet power expected by the Blandford-Payne mechanism for a standard accretion disk. This may imply that the accretion disks in most BL Lac objects (except the three sources) are

not standard thin disks.

If ADAFs are present in the BL Lac objects, there is a maximal jet power for a given black hole mass due to an upper limit on the accretion rate \dot{m}_{crit} for an ADAF (Narayan & Yi 1995). Compared with the standard disk case, ADAFs have much stronger magnetic field strength (Livio, Ogilvie, & Pringle 1999; Armitage & Natarajan 1999). We found in Fig. 2 that the power of jets in all sources is less than $0.01 L_{\text{Edd}}$. The power of the jets in most sources can be explained by the Blandford-Znajek mechanism if an ADAF is surrounding a rapidly spinning black hole at an accretion rate $\dot{m} = 0.01$, while six sources with jet power higher than the maximal jet power in the case of $a = 0.95$. The jets in these six sources may be powered by the Blandford-Payne mechanism from the ADAFs (e.g. ADIOS proposed by Blandford & Begelman 1999). Another possibility may be that the critical accretion rate \dot{m}_{crit} is higher than 0.01. If the critical accretion rate is 0.1, the power of jets in all sources can be explained in the frame of the Blandford-Znajek mechanism for ADAFs surrounding rapidly spinning black holes.

For given black hole mass, there is an upper limit on the optical continuum emission from an ADAF (Cao 2002a). As the radiative efficiency of ADAF is very low, even the maximal optical continuum luminosity of an ADAF is much fainter than the standard accretion disk at the same accretion rate. We test ADAF scenario in Fig. 3, and found that the pure ADAF model is unable to produce sufficient optical ionizing emission derived from [O II]-line emission for all sources (see the dash-dotted line in Fig. 3). The optical continuum emission from three sources 0828 + 493, 0851 + 202, and 2240 – 260 can be explained as emission from standard disks accreting at $\dot{m} = 0.01$ to 0.1 respectively, which is consistent with the fact that only the jets in these three sources may be produced by the Blandford-Payne mechanism for standard disks (see Fig. 1). For the remainder, we propose their optical continuum emission to be produced by the ADAF+SD systems. The optical continuum luminosity of the ADAF+SD system is available as a function of black hole mass m , while the accretion rate \dot{m} and the transition radius r_{tr} are specified. Such calculations presented in Fig. 3 show that the optical ionizing continuum emission from these BL Lac objects can be explained by the ADAF+SD model, if r_{tr} are in the range of 40 to 150 for $\dot{m} = 0.01$. We also calculate the cases of $\dot{m} = 0.1$, though it is still unclear whether an ADAF can exist in the inner region of the disk for such a high accretion rate. We find that the transition radii are in the range of 100 – 400 for $\dot{m} = 0.1$. The jets in these BL Lac objects may be accelerated by either the Blandford-Znajek mechanism or the Blandford-Payne mechanism (or by both two mechanisms) from the inner ADAF region, while the optical ionizing continuum emission is mainly from the outer standard disk region.

For adiabatic inflow-outflow solutions (ADIOSs) (Blandford & Begelman 1999), the

accretion rate of the disk is a function of radius r instead of a constant accretion rate along r for a pure ADAF. The ADIOS is described by the similar equations for an ADAF, while a r -dependent accretion rate $\dot{m}(r)$ is adopted instead. The accretion rate at the inner edge of the disk for an ADIOS should be at least as low as that required for pure ADAF solutions to keep the flow advection dominated. ADIOS has similar structure and a similar upper limit on the accretion rate at the inner edge of the disk as that of a pure ADAF, if the wind is not strong (Chang, Choi, & Yi 2002). In the case of strong winds, the gas swallowed by the black hole for an ADIOS is only a small fraction of the rate at which it is supplied, as most of the gas is carried away in the wind before it reaches the black hole. The maximal accretion rate of an ADIOS at its inner edge is significantly lower than that for a pure ADAF, if a strong wind is present. The maximal jet power extracted from a spinning black hole by the Blandford-Znajek mechanism for ADIOS cases should therefore be lower than that for pure ADAF cases. So, the power extracted from rapidly spinning black holes for ADIOS cases is insufficient for strong jets in some BL Lac objects.

Recently, Yuan (2001) proposed that a hot luminous disk may be present if the accretion rate is higher than the critical value \dot{m}_{crit} of the ADAF. This hot luminous disk may exist even if the accretion rate \dot{m} is as high as unit. The disk is much luminous than a pure ADAF due to its higher accretion rate and accretion efficiency. Thus, the maximal jet power $L_{\text{BZ}}^{\text{max}}$ extracted from a spinning black hole surrounded by such a hot luminous disk may be higher than that for a pure ADAF. This may be helpful to account for high power of jets in some BL Lac objects. The hot luminous disk has lower accretion efficiency than the standard thin disk. The optical continuum emission of these sources can be mainly from the standard disk region, if the hot luminous disk transits to a standard disk in the outer region of the disk. Such a hot luminous disk+SD model may work in some BL Lac objects.

We have adopted $f = 1$ in the normalization of the jet power estimate. In order to explore the case of f greater than unit, we perform calculations for $f = 10$ in Figs. 4 and 5. In this case, the jets in all sources cannot be accelerated by the standard magnetized disks. Only the Blandford-Payne mechanism for ADAFs (or ADIOSs) accreting at high rates around ~ 0.1 are able to produce strong jets in some sources. Even if this is the case, standard disks in the outer regions of the disks are still required to produce their optical ionizing luminosity (see Fig. 3).

In this paper, the accretion rate \dot{m} is adopted as a free parameter to compare our calculations with observations. For an accretion rate \dot{m} being less than 0.01 is adopted, for example $\dot{m} = 0.001$, we find that pure standard accretion disks are required to explain their optical continuum emission at least for some sources, i.e., the sources locate between the lines of $\dot{m} = 0.001$ and 0.01 in Fig. 3. However, the standard magnetized thin disks are not able

to fuel the jets in these sources (see Fig. 1 for $f = 1$ and Fig. 4 for $f = 10$). This indicates that the accretion rates \dot{m} , at least in these sources, should be around $\sim 0.001 - 0.01$. It means that the inner region of the disk would be advection dominated if $\dot{m} \sim 0.001 - 0.01$, which may imply that the critical accretion rate \dot{m}_{crit} is probably less than $\sim 0.001 - 0.01$ at least for these sources. The ADAF+SD scenario presented in this work is in general consistent with the models recently proposed for disk-jet connection in AGNs (Hujeirat et al. 2003; Livio, Pringle, & King 2003; Falcke, K rding, & Markoff 2003).

The transition radius r_{tr} is another parameter adopted in our calculations of the continuum emission from the disks. One possible mechanism for the transition might be the evaporation of the disk (Meyer & Meyer-Hofmeister 1994; Liu et al. 1999; R za nska & Czerny 2000; Meyer-Hofmeister & Meyer 2001). In this model, the disk-corona structure gradually changes to a pure vertically extended coronal or ADAF in the inner region of the disk. In the outer region of the disk, the cold disk and the hot corona above are in pressure equilibrium. In this scenario, most gravitational energy of the accretion matter is released in the hot corona (Haardt & Maraschi 1991; Kusunose, & Mineshige 1994; Svensson, & Zdziarski 1994). A small fraction of the soft photons from the cold disk is Compton up-scattered to X-ray photons by the hot electrons in the corona. Roughly about half of the scattered X-ray photons illuminate the cold disk (Haardt & Maraschi 1991; Nakamura & Osaki 1993; Cao et al. 1998; Kawaguchi, Shimura, & Mineshige 2001). Most soft photons from the disk leave the system without being scattered in the corona, and they are observed as optical/UV continuum. The cold disk in the disk-corona system has roughly about half brightness of a standard disk without a corona, if they are accreting at the same rate (Haardt & Maraschi 1991). The optical emission is therefore mainly from the cold disk, and the contribution to the optical emission from the corona and ADAF in the inner region of the disk can be neglected. If the disk-corona structure extends to the inner edge of the disk, the cold disk in the disk-corona is too bright to explain the ionizing luminosity of most BL Lac objects in this sample.

I thank the referee for his helpful comments and suggestions. This work is supported by NSFC(No. 10173016) and the NKBRSF (No. G1999075403). This research has made use of the NASA/IPAC Extragalactic Database (NED), which is operated by the Jet Propulsion Laboratory, California Institute of Technology, under contract with the National Aeronautic and Space Administration.

REFERENCES

- Antonucci, R. R. J., & Ulvestad, J. S., 1985, *ApJ*, 294, 158
- Armitage P. J., 1998, *ApJ*, 501, L189
- Armitage P.J., & Natarajan P., 1999, *ApJ*, 523, L7
- Augusto, P., Wilkinson, P. N., & Browne, I. W. A., 1998, *MNRAS*, 299, 1159
- Barth, A. J., Ho, L. C., & Sargent, W. L. W., 2002, *ApJ*, 566, L13
- Barth, A. J., Ho, L. C., & Sargent, W. L. W., 2003, *ApJ*, 583, 134
- Begelman M. C., Blandford R. D., & Rees M. J., 1984, *Rev. Mod. Phys.*, 56, 255
- Blandford R.D., & Begelman M.C., 1999, *MNRAS*, 303, L1
- Blandford R. D., & Payne D. G., 1982, *MNRAS*, 199, 883
- Blandford, R. D., & Znajek, R. L., 1977, *MNRAS*, 179, 433
- Cao, X., 2002a, *ApJ*, 570, L13
- Cao, X., 2002b, *MNRAS*, 332, 999
- Cao, X., Jiang, D.R., You, J.H., Zhao, J.L., 1998, *A&A*, 330, 464
- Cao, X., & Rawlings, S., in preparation
- Cao, X., & Spruit, H., 2002, *A&A*, 385, 289
- Cassaro, P., Stanghellini, C., Bondi, M., Dallacasa, D., della Ceca, R., & Zappal, R. A., *A&AS*, 139, 601
- Cavaliere, A., & D’Elia, V., 2002, *ApJ*,
- Chang H.Y., Choi C.S., & Yi I., 2002, *AJ*, 124, 1948
- Chiaberge, M., Capetti, A., Celotti, A., 1999, *A&A*, 349, 77
- Chiang, J., 2002, *ApJ*, 572, 79
- Esin, A. A., McClintock, J. E., & Narayan, R., 1997, *ApJ*, 489, 865
- Falcke, H., K rding, E., & Markoff, S., 2003, *A&A*, accepted (astro-ph. 0305335)

- Falomo, R., Kotilainen, J. K., & Treves A., 2002, *ApJ*, 569, L35
- Fan, J.H., 2003, *ApJ*, 585, L23
- Ferrarese, L., & Merritt, D., 2000, *ApJ*, 539, L9
- Francis P.J., Hewett P.C., Foltz C.B., Chaffee F.H., Weymann R.J., Morris S.L., 1991, *ApJ*, 373, 465
- Gebhardt, K. et al., 2000, *ApJ*, 539, L13
- Ghisellini, G., Celotti, A., 2001, *A&A*, 379, L1
- Ghosh P., & Abramowicz M. A., 1997, *MNRAS*, 292, 887
- Haardt, F., & Maraschi, L., 1991, *ApJ*, 380, L51
- Hubeny, I., Blaes, O., & Krolik, J. H., Agol, E., *ApJ*, 559, 680
- Hujeirat, A., Livio, M., Camenzind, M., & Burkert, A., 2003, *astro-ph/0304085*
- Kaspi S., Smith P.S., Netzer H., Maoz D., Jannuzi B.T., & Giveon U., 2000, *ApJ*, 533, 631
- Kawaguchi, T., Shimura, T., Mineshige, S., 2001, *ApJ*, 546, 966
- Kusunose, M., & Mineshige, S., 1994, *ApJ*, 423, 600
- Laor A., & Netzer H., 1989, *MNRAS*, 238, 897
- Lawrence, C. R., Zucker, J. R., Readhead, A. C. S., Unwin, S. C., Pearson, T. J., Xu, W., 1996, *ApJS*, 107, 541
- Liu, B.F., Yuan, W., Meyer, F., Meyer-Hofmeister, E., & Xie, G.Z., 1999, *ApJ*, 527, L17
- Livio M., Ogilvie G. I., & Pringle J. E., 1999, *ApJ*, 512, 100(L99)
- Livio, M., Pringle, J.E., & King, A.R., *astro-ph/0304367*
- Lubow, S.H., Papaloizou, J.C.B., Pringle, J.E., 1994, *MNRAS*, 267, 235
- Mahadevan, R., 1997, *ApJ*, 477, 585
- McLure R.J., & Dunlop J.S., 2002, *MNRAS*, 331, 795
- Meyer, F., & Meyer-Hofmeister, E., 1994, *A&A*, 288, 175
- Meyer-Hofmeister, E., & Meyer, F., 2001, *A&A*, 380, 744

- Moderski R., & Sikora M., 1996, *A&AS*, 120, 591
- Murphy, D. W., Browne, I. W. A., & Perley, R. A., *MNRAS*, 264, 298
- Nakamura, K., & Osaki, Y., 1993, *PASJ*, 45, 775
- Narayan R., 2002, in *Lighthouses of the Universe: The Most Luminous Celestial Objects and Their Use for Cosmology*, Proceedings of the MPA/ESO/, p. 405
- Narayan R., & Yi I., 1995, *ApJ*, 452, 710
- Novikov I., & Throne K. S., 1973, in *Black holes*, eds de Witt C. and de Witt B., Gordon & Breach, New York(NT73)
- Ogilvie G.I., & Livio M., 1998, *ApJ*, 499, 329
- Ogilvie G.I., & Livio M., 2001, *ApJ*, 553, 158
- Press, W.H., Teukolsky, S.A., Vetterling W.T., & Flannery B.P., 1992, *Numerical recipes in FORTRAN: the art of Scientific computing*, Cambridge university press.
- Rawlings S., & Saunders R., 1991, *Nature*, 349, 138
- Rector, T. A., & Stocke, J. T., 2001, *AJ*, 122, 565
- Rees M. J., Begelman M. C., Blandford R. D., & Phinney E. S., 1982, *Nature*, 295, 17
- Romanova M. M., Ustyugova G. V., Koldoba A. V., Chechetkin V. M., & Lovelace R. V. E., 1998, *ApJ*, 500, 703
- Rózańska, A., & Czerny, B., 2000, *A&A*, 360, 1170
- Shu F.H., 1991, in Lambert D.L., ed, *Frontiers of stellar evolution*, Astronomical Society of the Pacific Conference Series (ASP), p.23
- Stickel, M., Fried, J. W., Kühr, H., 1989, *A&AS*, 80, 103
- Stickel, M., Fried, J. W., & Kühr, H., 1993, *A&AS*, 98, 393
- Svensson, R., & Zdziarski, A., 1994, *ApJ*, 436, 599
- Sun, W., & Malkan, M., 1989, *ApJ*, 346, 68
- Tadhunter, C. N., Morganti, R., di Serego-Alighieri, S., Fosbury, R. A. E., Danziger, I. J., 1993, *MNRAS*, 263, 999

- Tout C. A., & Pringle J. E., 1996, MNRAS, 281, 219
- Urry, C.M., & Padovani, P., 1995, PASP, 107, 803
- Urry, C. M., Scarpa, R., O’Dowd, M., Falomo, R., Pesce, J. E., & Treves, A., 2000, ApJ, 532, 816
- Veron-Cetty, M.P., & Veron, P., 2000, A&A Rev., 10, 81
- Wang, J.M., Staubert, R., & Ho, L.C., 2002, ApJ, 579, 554
- Willott, C.J., Rawlings S., Blundell K.M., & Lacy M., 1999, MNRAS. 309. 1017
- Wilson, A. S., & Colbert E. J. M., 1995, ApJ, 438, 62
- Yuan, F., 2001, MNRAS, 324, 119

Table 1. Data of BL Lac objects

Source	Redshift	$m_R(\text{host})$	$\log L_{[\text{O II}]}$	References	$\log L_{\text{ext},151}$	References	$\log M_{\text{bh}}/M_{\odot}$	$\log Q_{\text{jet}}$
0118–272	0.559	>17.96	27.21	C99	<9.49	36.86
0138–097	0.733	>18.38	34.71	RS01	26.94	C99	<9.60	36.62
0235+164	0.940	>17.35	35.35	S93	27.03	C99	<10.41	36.71
0426–380	1.030	18.50	27.50	C99	9.94	37.11
0521–365	0.055	14.35	33.64	T93	26.91	AU85	8.68	36.60
0537–441	0.896	>17.50	35.27 ^a	S93	27.77	C99	<10.28	37.34
0735+178	0.424	>19.50	26.11	C99	<8.40	35.91
0754+100	0.670	>17.09	27.03	M93	<10.14	36.71
0820+225	0.951	>19.38	33.29 ^a	S93	28.33	C99	<9.41	37.82
0823+033	0.506	>19.04	34.03	S93	25.59	C99	<8.83	35.47
0828+493	0.548	18.98	34.99	RS01	26.36	C99	8.95	36.13
0829+046	0.180	16.54	25.80	AU85	8.90	35.65
0851+202	0.306	>17.95	34.81 ^b	S89	25.66	C99	<8.79	35.53
0954+658	0.367	>18.85	34.24	RS01	26.12	C99	<8.55	35.93
1144–379	1.048	>19.93	34.57 ^a	S89	26.58	C99	<9.25	36.32
1418+546	0.152	15.87	34.07	S93	25.46	C99	9.04	35.36
1538+149	0.605	18.73	34.64	S93	27.43	C99	9.20	37.04
1749+096	0.320	18.15	33.88	S93	24.52	M93	8.75	34.55
1749+701	0.770	>16.92	35.20	S89	26.37	C99	<10.39	36.13
1803+784	0.684	>19.15	34.88 ^b	L96	26.81	C99	<9.13	36.51
1807+698	0.051	13.54	34.11	S93	25.83	C99	9.00	35.67
1823+568	0.664	18.57	35.02	S93	27.87	C99	9.39	37.42
2007+777	0.342	18.02	34.02	S89	26.14	C99	8.89	35.94
2131–021	1.285	>18.50	35.16	RS01	28.04	C99	<10.21	37.57
2200+420	0.069	14.55	33.07 ^b	S93	24.69	C99	8.83	34.70
2201+044	0.027	13.50	24.15	A98	8.32	34.23
2240–260	0.774	>20.22	35.52	S93	27.81	C99	<8.74	37.38
2254+074	0.190	16.07	33.27 ^b	S93	25.22	C99	9.19	35.15

^aconverted from Mg II

^bconverted from [O III].

Note. — Column (1): source name; Column (2): redshift; Column (3): R -band magnitude of the host galaxy; Column (4): narrow-line luminosity $L_{[\text{O II}]}$ (W); Column (5): references for $L_{[\text{O II}]}$; Column (6): extended radio luminosity at 151 MHz in the rest frame of the source (W Hz^{-1}); Column (7): references for $L_{\text{ext},151}$; Column (8): black hole mass; Column (9): jet power (W).

References. — AU85: Antonucci & Ulvestad (1985); C99: Chiaberge, Capetti, & Celotti (1999); L96: Lawrence et al. (1996); M93: Murphy, Browne, & Perley (1993); RS01: Rector & Stocke (2001); S89: Stickel, Fried, & Kühr (1989); S93: Stickel, Fried, & Kühr (1993); T93: Tadhunter et al. (1993);

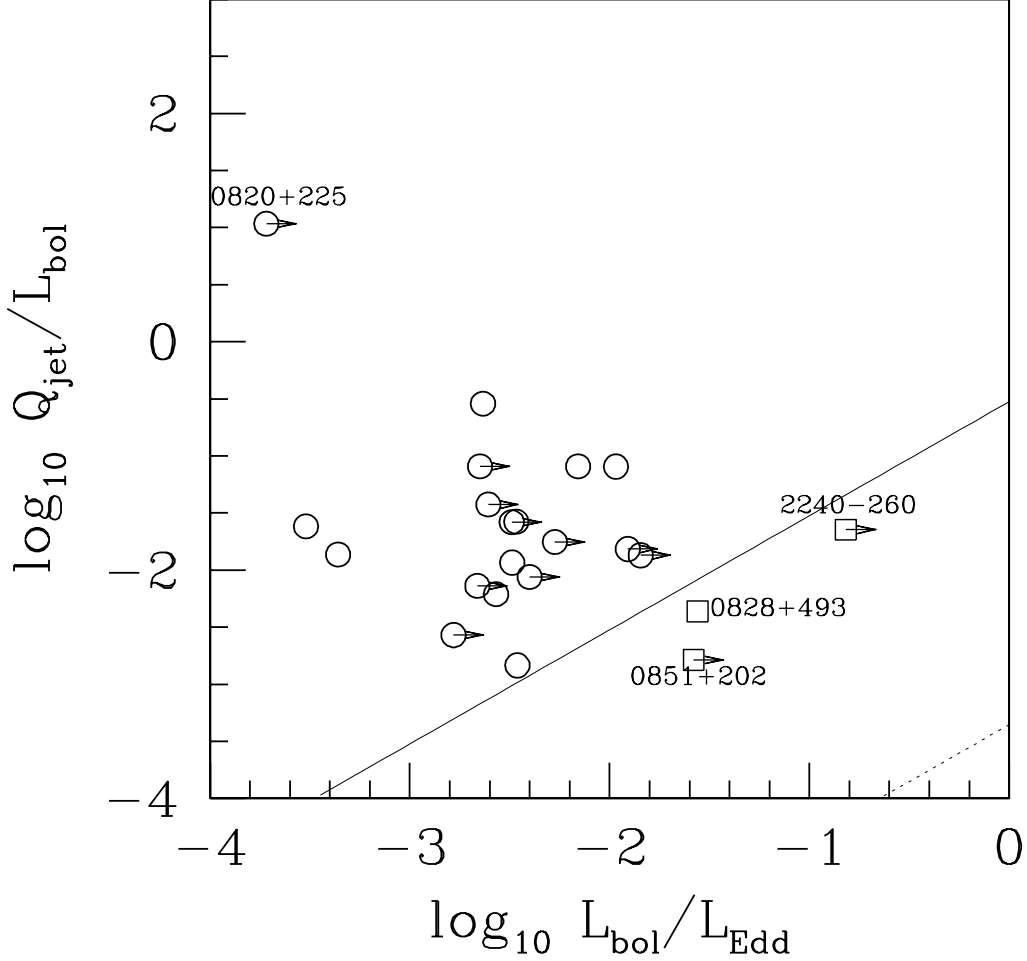


Fig. 1.— The ratio $L_{\text{bol}}/L_{\text{Edd}}$ versus the ratio $Q_{\text{jet}}/L_{\text{bol}}$ ($f = 1$ is adopted). The solid line represents the maximal jet power $L_{\text{BP}}^{\text{max}}$ extracted from a standard accretion disk (the Blandford-Payne mechanism), while the dotted line represents the maximal jet power $L_{\text{BZ}}^{\text{max}}$ extracted from a rapidly spinning black hole $a = 0.95$. The sources below the solid line are labelled as squares.

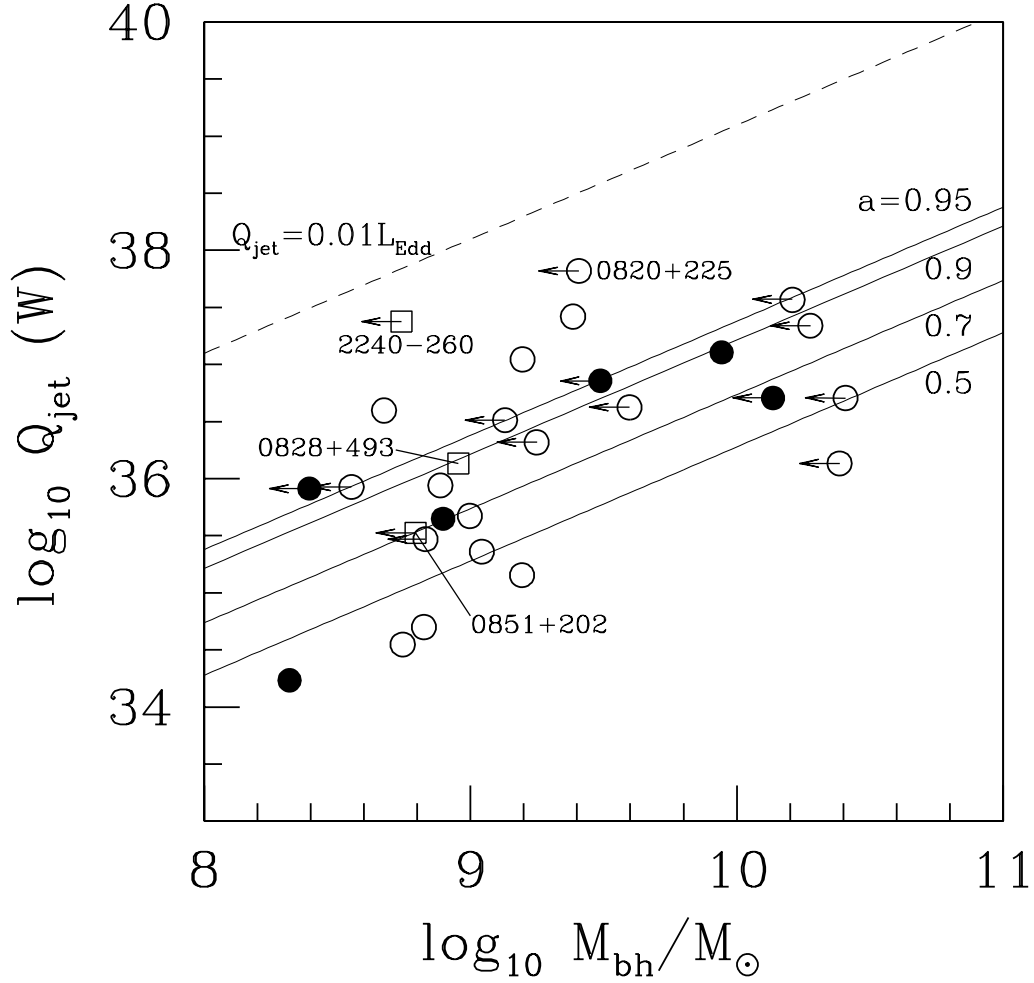


Fig. 2.— The black hole mass M_{bh} versus jet power Q_{jet} ($f = 1$ is adopted). The full circles represent the sources without emission line data. The solid lines represent the maximal jet power $L_{\text{BZ}}^{\text{max}}$ extracted from the spinning black holes surrounded by ADAFs as functions of M_{bh} for different values of spin a , respectively ($\dot{m}_{\text{crit}} = 0.01$ is adopted). The dashed line represents the jet power $Q_{\text{jet}} = 0.01 L_{\text{Edd}}$.

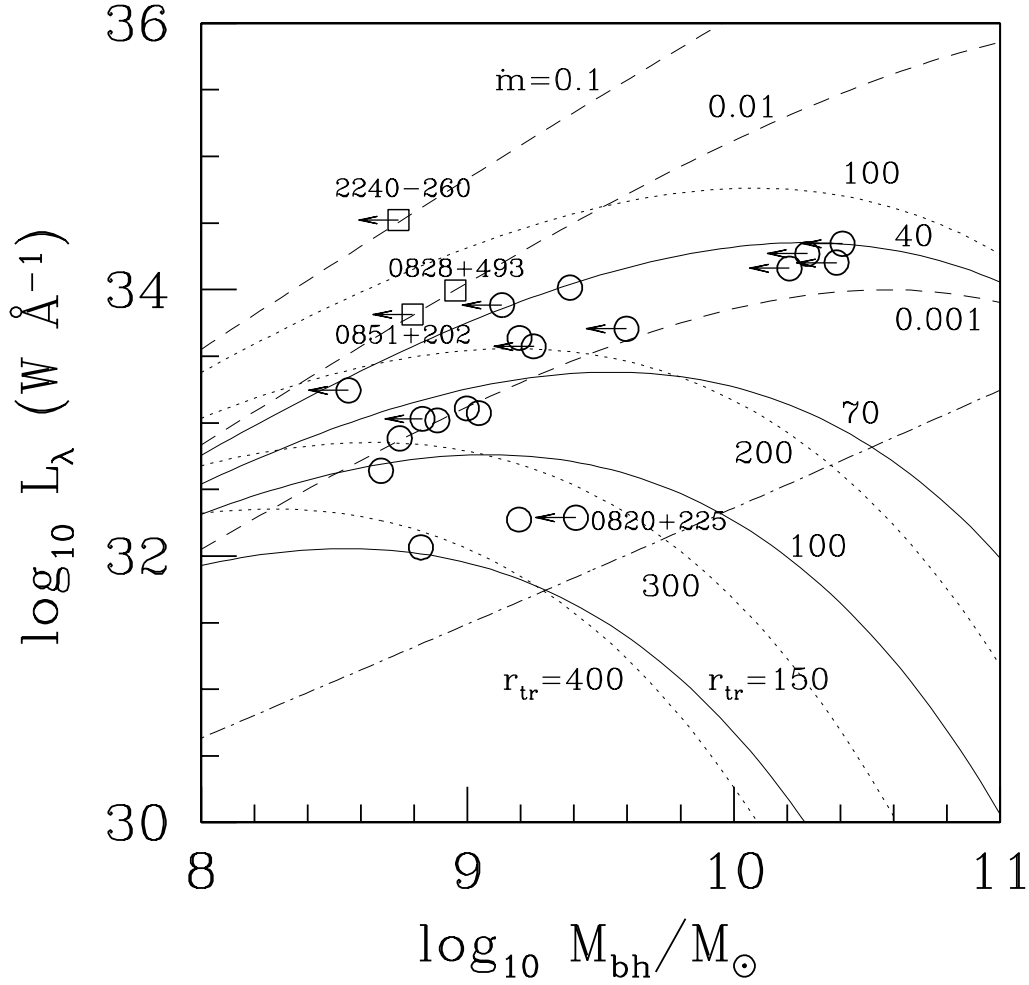


Fig. 3.— The black hole mass M_{bh} versus optical luminosity L_{λ} at 3727 \AA . The solid lines represent for ADAF+SD models with different transition radii r_{tr} for $\dot{m} = 0.01$, while the dotted lines represent the cases of $\dot{m} = 0.1$. The dashed lines represent standard accretion disks with $\dot{m} = 0.001, 0.01$, and 0.1 , respectively. The dash-dotted line is the maximal optical luminosity as a function of black hole mass M_{bh} for the pure ADAF case.

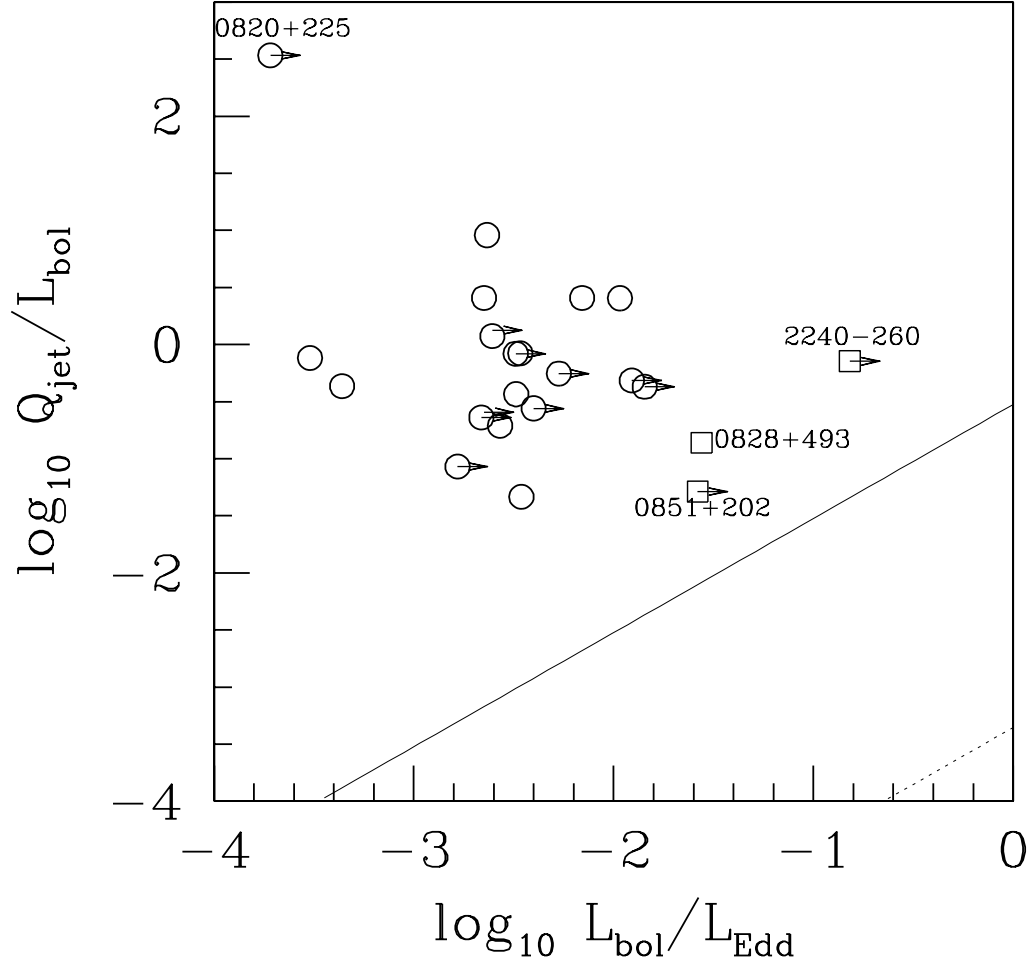


Fig. 4.— Same as Fig. 1, but $f = 10$ is adopted.

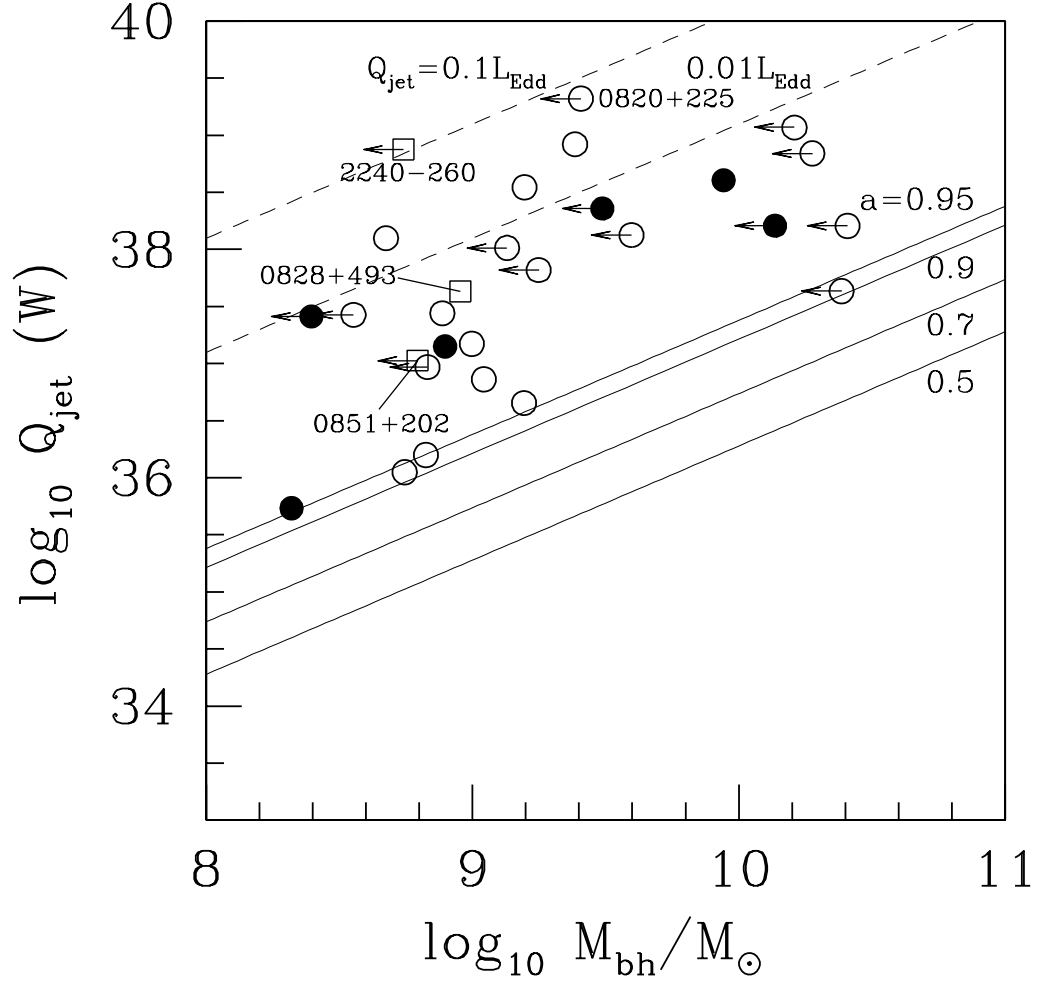


Fig. 5.— Same as Fig. 2, but $f = 10$ is adopted.